

Molecular Dynamics of Kuhn and Grün Chain Segments Applied to the Mechanical Behavior of Polymer Fibers

Hawthorne Davis

College of Textiles, North Carolina State University, P.O. Box 8301,
Raleigh, North Carolina 27695-8301

Received April 5, 1993; Revised Manuscript Received October 31, 1994*

ABSTRACT: A molecular dynamics simulation for a Kuhn and Grün polymer chain segment has been developed and compared with the theory. Agreement of the computer experiments and theory, including a short-chain adaptation of the theory due to Weiner, was for practical purposes exact. The work discovered that due to the basic assumption and inextensible bonds temperature, or thermal energy, is not isotropic in a Kuhn and Grün chain segment. This anisotropy increases with the relative extension r/nl . This should not occur in a real material, which is held together by potential energy rather than by mathematical constraints. In this regard, therefore, this theory, and possibly any theory which depends on fixed-length interatomic bonds, may not be a good approximation to reality with varying chain extension. Introducing a harmonic potential function which maintains the angle between bonds close to an equilibrium value θ_0 , changes the force/extension relation of a chain segment such that the end-to-end length of the segment is finite at zero force. This modification, however, did not eliminate the anisotropic temperature problem caused by inextensible bonds.

Introduction

Synthetic fibers are complex, anisotropic networks of polymer molecules.¹ The entire structure consists of finite length, e.g., $\sim 1 \mu\text{m}$, un-cross-linked molecules. The stable nodes in this network are places where molecule segments have agglomerated in a coherent or orderly fashion. These are called crystalline regions in fibers. The network connectives therefore are what is left, i.e., segments of polymer molecules which are connected to two nodes. The ends of connective chain segments are immobilized, a fact which makes their dynamics different from those of free polymer molecules. Although fiber microstructure is complicated, it has been shown from structural studies by Nakamae et al.² and from analysis of mechanical behavior by Prevorsek³ that the nodes and connective chain segments are functionally in series in partly crystalline fibers. Understanding the dynamics of these connective segments, in particular the effects of temperature and of any constraints imposed on them, e.g., by the structure, is essential to understanding fiber properties and behavior. Connective regions might also contain two types of entities which do not connect anything. These have been called cilia and floating chains⁴ and would have dynamic behavior somewhat like a free polymer molecule. These will not be discussed further here, since by assumption they are disconnected from the network of interest.

The analog in fiber science of the ideal polymer molecule of polymer physics is the Kuhn and Grün (K/G)⁵ chain segment. This model is a chain of inextensible "bonds" connected by freely rotating "swivel" joints. The ends of the chain are fixed in space. It might be expected that the K/G theory would be for fiber science what the Gaussian chain segment has been for polymer physics; i.e., it should give reasonable explanation of fiber properties at least in the rubbery regime. Davis⁶ attempted to understand the rubbery regime dynamic mechanical properties of fibers with K/G chain segments, and while there was limited success, there appear to be significant problems which are inherent

to assumptions in the theory. A more realistic chain segment model is needed, but 50 years after the original problem was solved, one does not exist in an analytic form. There have, however, been attempts to understand the dynamic behavior of chain segments using molecular dynamics computer calculations.

Weiner and Stevens⁷ modeled a chain segment of 10 atoms connected by stiff springs and studied the effect on the retractive force/extension relationship of confining planes perpendicular to the end-to-end chain (chain) vector. Weiner and Berman⁸ used a similar model to study the effect on the retractive force of a large (relative to bond length) confining tube having its axis along the chain vector. While neither of these exactly represents a K/G chain segment, the work is important for fibers because it focuses on constraints expected to affect the behavior of connectives. Winker and Reineker⁹ studied the dynamics of short, 3-5 atom, chain segments, where the motion of the atoms was confined to the plane normal to the chain vector. While they were mainly interested in the chaotic fluctuation of retractive force, they did produce force/extension relationships.

Molecular dynamics calculations to be described here were carried out in an effort to substitute the desired analytic theory with a computer simulation. While real chain segments have valence bonds and rotational barriers, which are missing from the K/G chain, the K/G limiting case was modeled and compared with the available statistical mechanics theories to check on the rest of the modeling.

Kuhn and Grün Chain Segment

The K/G theory for a chain segment is elegant and simple. While, as indicated by Flory,¹⁰ it contains a uniqueness assumption about the end-to-end chain vector, which makes it inapplicable to a segment of a rubbery network or a longer molecule, it appears to be perfectly adapted to the network of a semicrystalline fiber, which is made of chain segments having their ends immobilized by crystals. This theory predicts for a set of n rigid bonds of length l connected into a chain by unhindered "swivel joints" two key properties. One property is the tension F required to maintain an

* Abstract published in *Advance ACS Abstracts*, December 15, 1994.

extension r/nl , where r is the end-to-end length, at absolute temperature T . This theory is thus based on strain-ensemble statistics. The relationship is

$$F = kT/l \mathcal{L}^{-1}(r/nl) \quad (1)$$

where \mathcal{L}^{-1} represents the inverse of the Langevin function. Note that F is greater than 0 so long as the two ends of the segment are not coincident. Another property defined by this theory is a relationship between $\langle \cos \Theta \rangle$, which is the same as r/nl , and $\langle \cos^2 \Theta \rangle$, which would otherwise be linearly independent. If $f_{\text{am}} \equiv \frac{3}{2} \langle \cos^2 \Theta \rangle - \frac{1}{2}$, this relationship is given by

$$r/nl = \mathcal{L}(3r/nl)(1/(1 - f_{\text{am}})) \quad (2)$$

The theory uses Stirling's formula to approximate the degeneracy and therefore is expected to be exactly correct only for long chains. Weiner¹¹ calculated the retractive force for short chains using similar assumptions. Note that f_{am} is zero unless tension is applied to the ends of a K/G chain segment.

Amorphous Orientation Function in Fibers

A fiber is often described by its crystalline and noncrystalline orientation functions and the fraction X of the fiber which is crystalline. The average "orientation" of the noncrystalline fraction is f_{am} defined above. A similar orientation function can be defined for the crystalline regions. Fibers, e.g., poly(ethylene terephthalate) fibers, can be made with high orientation and low crystallinity. These are, however, not stable and will tend to crystallize until X is about 0.5. Let us for now be concerned only with this relatively stable, half-crystalline state.

f_{am} is usually measured by determining the total anisotropy of a fiber optically and subtracting the crystalline contribution based on X-ray measurements. The procedure has been discussed in detail by Samuels.¹² f_{am} is formally a measure of spatial orientation. Its relationship to r/nl , which is the ratio of chain vector length r to contour length nl , a different kind of orientation, is determined by the statistical mechanics, which are model dependent. After early work by Samuels,¹³ f_{am} has come to be fairly accepted for fibers as a state parameter representative of r/nl . Fibers reportedly can have high, e.g., 0.7,¹⁴ f_{am} even after they have been completely relaxed. This important behavior must originate in a property of real molecule segments which is different from K/G segments.

Computer Modeling a Kuhn and Gr \ddot{u} n Chain Segment

Description of Model. A molecular dynamics computer simulation for a K/G chain segment extended along the z -coordinate axis was developed. The model consisted of noninteracting "atoms" of mass 14 amu connected into a chain by inextensible bonds. The end atoms of the chain were immobilized by setting the reciprocal of their masses to zero. The distance between any two neighboring atoms in the chain was maintained constant to within 10^{-6} (relative) with an iterative constraints algorithm.¹⁵ The atoms in the chain were given random initial velocities corresponding with zero net momentum and a certain temperature T . The model was integrated with the Verlet leapfrog algorithm. The model was run at constant energy, which also corresponded with constant temperature, since by

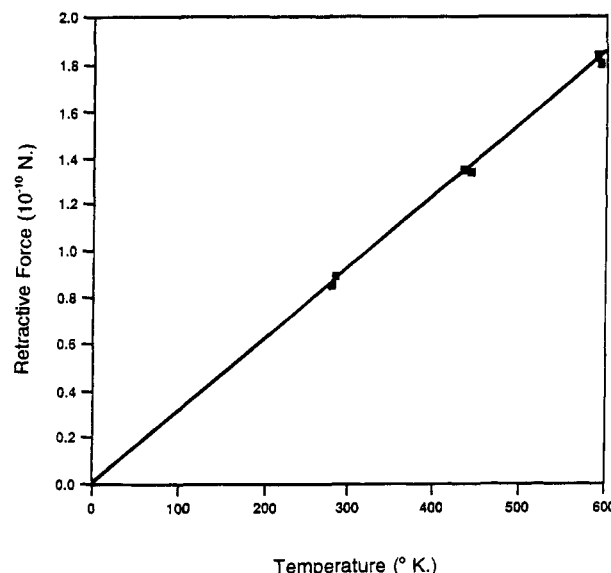


Figure 1. Temperature dependence of chain segment retractive force from molecular dynamics model, $r/nl = 0.72$; from least squares, slope = 3.1×10^{-13} N/K, intercept = 6.3×10^{-14} N.

definition there were no changes in potential energy. Energy conservation was typically 10^{-7} (relative) in 100 ps, with 3 fs time steps. The retractive force in the chain was taken as the time average of the difference in the z component of the force on the two end atoms. In this model, the only contribution to this force is from the bond length constraint. $\langle \cos^2 \Theta \rangle$ and the second moment of the velocity distribution were calculated by sampling the bond angles and velocities at random times amounting to 20% of the total time. The retractive force was sampled on every time step for averaging. Before any statistical data were collected, the model was run at constant energy for at least 100 ps to allow the velocity distribution to approach Maxwell-Boltzmann. Typically, the ratio $\langle v^2 \rangle^{1/2} / \langle v \rangle$ for this model was 1.095 ± 0.001 . This ratio for a Maxwell-Boltzmann distribution is 1.0854. In examining the results which follow, it will be apparent that this difference is not important.

Results

The figures below compare results from this model with the K/G theory and modifications thereof. Figure 1 shows that the tension produced by the chain is proportional to absolute temperature, as in the theory. The six data points shown were derived from a chain with 101 (99 mobile) atoms. The points represent one cycle of heating and cooling. The retractive force extrapolates to zero at absolute zero, and the slope is $(k/l \mathcal{L}^{-1}(r/nl))$, as is required by the theory.

Figure 2 compares the dependence of retractive force on r/nl for a 101 atom chain with the K/G theory at the same temperature. For practical purposes, agreement is exact. Note, however, that there are no data points for $r/nl > 0.85$. This is because the bond constraints cannot conveniently be satisfied beyond this extension with the algorithm used.

Figure 3 compares the retractive forces for chains of different lengths. It can be seen that at a given value for r/nl shorter chains develop lower retractive force. The solid curve in Figure 3 is calculated from a theory due to Weiner.¹⁰ The computer model agrees almost perfectly with this theory.

Figure 4 compares computed values for $(1 - \langle \cos^2 \Theta \rangle)$ for a 101 atom chain with the same parameter derived

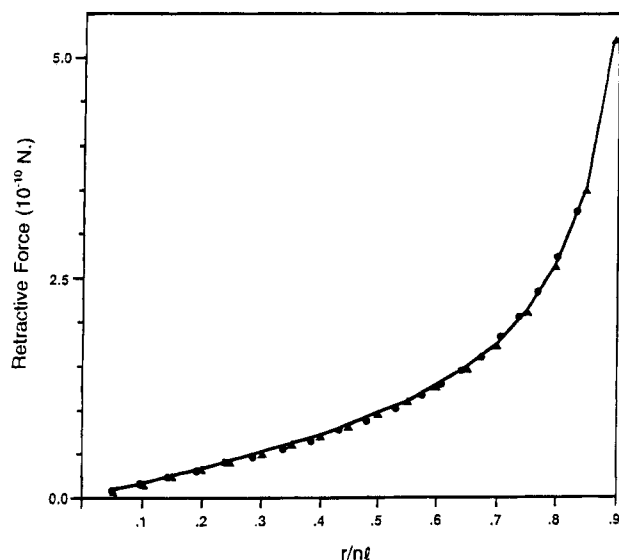


Figure 2. Comparison of force/extension relationships for molecular dynamics model with K/G chain segment: (○) molecular dynamics; (▲) K/G theory. Temperature = 573 K, $l = 1.53$ Å.

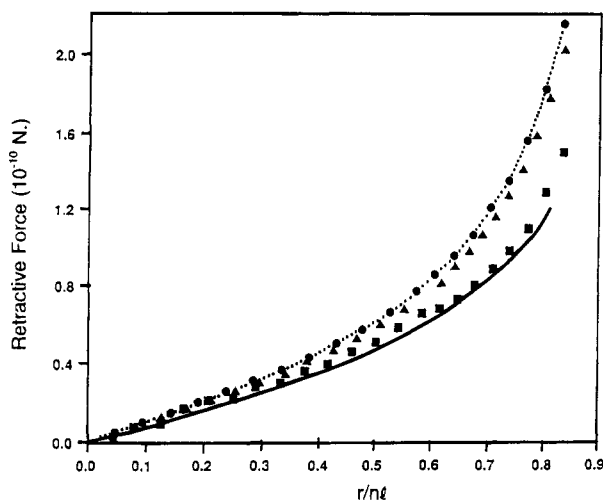


Figure 3. Effect of chain segment length on retractive force: (■) 4 mobile atoms; (▲) 24 mobile atoms; (●) 99 mobile atoms. The curve is from Weiner.¹¹ Temperature = 573 K.

from the K/G theory. Again the agreement is completely satisfactory.

The Network Collapse Problem As Applied to Fibers

General. A K/G chain segment generates a retractive force so long as the ends of the segment are separated by a finite distance. A network of these segments would therefore tend to collapse under zero force. Weiner and Stevens⁷ showed that confining chain segments between two planes, e.g., the lamellae in a crystalline polymer, would prevent this collapse.

Typical fibers, e.g., polyester fibers, are believed to have stable, high amorphous orientation under zero force. For example, Samuels¹⁶ indicated that a polyester fiber could have f_{am} as high as 0.83, which in K/G theory corresponds with r/nl of 0.94. Even after complete relaxation at high temperature, f_{am} remains as high as 0.7, corresponding with r/nl of 0.89. Here is an extreme example of lack of collapse. In addition to the Weiner and Stevens suggestion, two further mechanisms for preventing collapse, which are qualitatively consistent

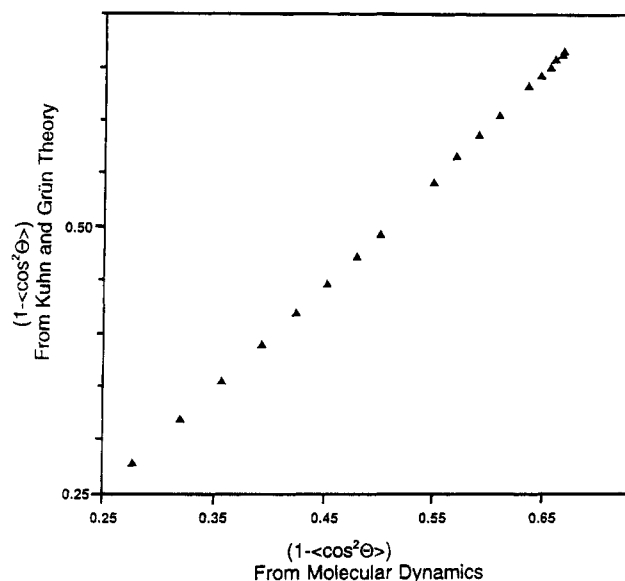


Figure 4. Comparison of orientation functions $(1 - \langle \cos^2 \Theta \rangle)$ from K/G theory and from molecular dynamics model.

with the high amorphous orientations observed in fibers, were identified in this work.

Confined Chain Segments. It is possible to conceptualize a model consistent with the K/G theory which will predict, using reasonable assumptions, that non-crystalline f_{am} values as reported could be stabilized using only repulsive forces without the Weiner/Stevens interaction mentioned above. The idea is as follows: Since noncrystalline chain segments are confined by having their ends embedded in a crystal, they are forced to interact, at least repulsively, with their neighbors. It is something like each chain segment is confined to a tube, the average volume of which is determined by the density of the noncrystalline regions.

A computer model was developed by enclosing a K/G chain segment in a cylindrical tube, the axis of which is the end-to-end vector of the chain segment. The radius of the tube is coupled to r/nl such that the tube has a constant volume. In the model each atom sees a radial force, derived from the repulsive part of a Lennard-Jones potential, which pushes it toward the axis of the tube. It was a little difficult to get this model to run because of the high forces produced by the tube; however, eventually the results shown in Figure 5 were obtained. Two different tubes were tested. When the chain segment was fully extended ($r/nl = 1$), one tube had a diameter which was 5 Å (3.3 l) and the other was 2.5 Å (1.6 l). Fair, qualitative agreement between model and a simple theory¹⁷ adapted from polymer physics is suggested in Figure 5; however, it is not clear how to parametrize the theory so that it can be compared with the model quantitatively. It is also not clear exactly how to relate the tube diameter to structural parameters of a real material.

Unexpected, jumprope-like correlated motion was encountered with tube-confined chain segments. This was discovered from moving pictures made by saving the coordinates of each "atom" after each 5 time steps. It is not known whether this correlated motion, which was not apparent without the tube, causes a significant change in retractive force. Superimposing a small, random fluctuation on the effective tube radius did not change this motion significantly.

Internal Chain Stiffness. Simple chain stiffness can be produced by a potential function which maintains

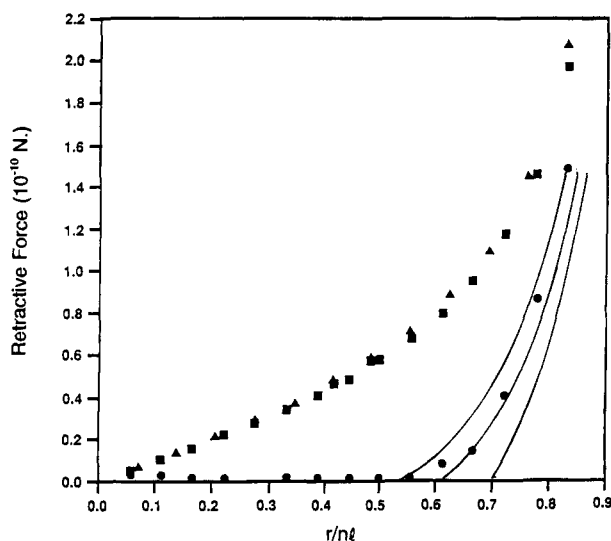


Figure 5. Effect of tube constraint on chain segment retractive force: (Δ) no tube; (\blacksquare) tube diameter = $3.3l$; (\bullet) tube diameter = $1.6l$. Curves are from theory discussed in ref 17.

the angle between two sequential main chain bonds close to a certain angle Θ_0 . This characteristic was implemented in the molecular dynamics model by means of the potential function

$$V = K/2(\cos \Theta - \cos \Theta_0)^2 \quad (3)$$

where Θ represents the instantaneous value of the angle between two consecutive bonds. Otherwise, the chain segment is like a K/G segment; viz., it has inextensible main chain bonds and it can penetrate itself. To simulate a hydrocarbon chain, K would be set to about 1.35×10^{-15} J. For a K/G chain, K would be zero. For the valence angle chain the fully extended length is $(nl)/\langle \sin \Theta_2 \rangle$. Since increasing tension on a chain segment, e.g., by increasing r/nl , would tend to increase $\langle \Theta \rangle$, the effective fractional extension depends on force and thus on intended fractional extension. To simplify the current discussion, fractional extension was defined as r/L , where $L = nl \sin \Theta_0/2$. Θ_0 is 113° for $K \neq 0$ and 180° for $K = 0$. A time-averaged value of Θ was also calculated and used to compute a "true" fractional extension. This correction changes the details but not the overall impression of the following figures and will be ignored in the current discussion. Figure 6 compares retractive force vs r/L for a range of K values. It can be seen that increasing chain stiffness causes the retractive force to pass through zero at higher values of r/L . Although it may not be apparent in the figure, the modulus of, e.g., a fiber, which is a network of these chain segments, would be limited by the valence bond stiffness. All of the MD calculations were done at constant energy after the model had been conditioned at a constant 573 °K. The average temperature over a run was usually within a few degrees of this designed value, and no attempt was made to implement a correction.

Discussion

The close agreement of theory and computer model found here is superficially not surprising. There has been work, e.g., by Helfand¹⁸ or Fixman and Kovac,¹⁹ which shows that the statistical mechanics of systems containing constrained bonds is different from that of the same systems containing stiff elastic bonds. No

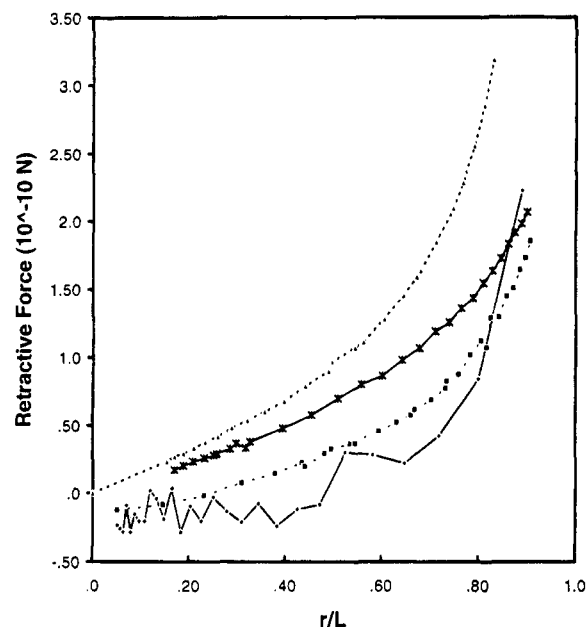


Figure 6. Retractive force vs r/L (see text for definition) for chain segment with valence bond bending potential function: (\diamond) $K = 1.35 \times 10^{-15}$ J; (\blacksquare) $K = 1.35 \times 10^{-16}$ J; (\times) $K = 1.35 \times 10^{-17}$ J; (Δ) $K = 0$.

problem was expected from this here, because the work sought to compare the same system of constrained bonds from two different points of view. It should be pointed out, however, that the statistical mechanics theory⁵ is based on *a priori* probability for spatial orientation of bonds, while the computer model is based on Newtonian mechanics of particles subjected to specific constraints. Here *a priori* means that the probability for a particular bond to make an angle $\Theta \pm d\Theta/2$ with the end-to-end vector depends on the amount of space available around Θ , i.e., $2\pi \sin \Theta d\Theta$, and the auxiliary conditions of constant end-to-end length and constant number of bonds.

One of the reviewers of this paper pointed out that the existence of constraints can effect an equilibrium probability distribution function which is not immediately obvious. For example, Hoover²⁰ showed that, for a flexible, triatomic molecule with fixed length bonds in two dimensions, there is an unexpected, preferred angle of $\pi/2$ between the bonds. Thus it is possible that the probability distribution, assumed in the K/G analysis, differs from that which obtains in the molecular dynamics, which presumably is correct for the constrained bond model within the accuracy of the computations and the integration algorithm.

The dependence of the probability distribution for polar angle θ on the fractional extension (r/nl) was derived in the K/G paper⁵ and can be obtained from the molecular dynamics simulation. It is most convenient to work with the distribution $P(\cos \theta)$. From ref 5

$$P(\cos \theta) = Z \exp\{\mathcal{L}^1(r/nl) \cos \theta\} \quad (4)$$

where Z is a normalizing factor. $P(\cos \theta)$ was determined with the molecular dynamics by collecting values of individual bond $\cos \theta$'s, sampled at random times amounting to 20% of the total time, into 100 bins (uniformly distributed in $\cos \theta$) for different values of r/nl . Figure 7 compares $P(\cos \theta)$ obtained by these two methods at three values of r/nl . In all cases the results were scaled so that $\int P(\cos \theta) d \cos \theta = 1$. The results from molecular dynamics and the theory match so

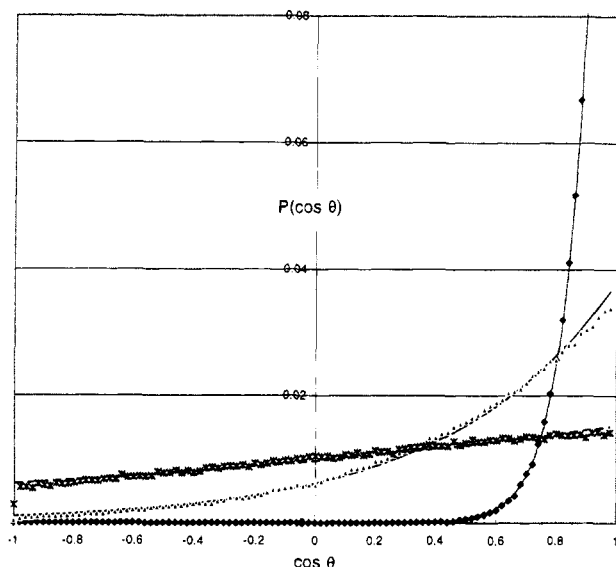


Figure 7. Probability distribution for angle (θ) between individual bonds and the 101 atom chain segment end-to-end vector presented as a function of $\cos \theta$. Lines are K/G theory. Data points are from molecular dynamics model: (*) $r/nl = 0.15$; (▲) $r/nl = 0.50$, (◆) $r/nl = 0.92$.

closely that it may not be possible to distinguish the theoretical "lines" from the molecular dynamics "data points". From this it must be concluded that a more rigorous analysis would not change the K/G probability distribution significantly. The probability distribution for the angle between adjacent bonds is almost the same as that shown in Figure 7, except that the values for $\cos \theta$ must be replaced by $-\cos \theta$. The distribution of the intrabond angle is not given in the K/G theory.

Working with this model pointed out two related problems which affect the usefulness of the K/G theory for quantitatively representing real polymer chain segments. The first of these involves the fact, mentioned earlier and dealt with in refs 18–20, that the equilibrium statistics of a constrained bond system differ from those for an elastic bond system in the limit of infinite bond stiffness. The second, which is one way that the result of constrained bonds is manifested in the dynamics of a system, involves thermal energy partitioning and appears not to have been noticed previously. Figure 8 shows how an anisotropy in temperature, represented as $\langle V^2 \rangle / \langle V_{xy}^2 \rangle$, changes with r/L . $\langle V^2 \rangle / \langle V_{xy}^2 \rangle$, ignoring fluctuations due to finite sampling, should have the value 1.5 independent of r/L . With increasing r/L , however, thermal energy becomes increasingly concentrated in the xy plane. This apparently occurs because relative motion of two sequential atoms is not possible in the direction of the constrained bonds. A similar effect was observed in both K/G and valence bond chain segments. This would not occur, i.e., temperature would be isotropic, in a real chain of atoms having "bonds", which are actually potential wells in which atoms can vibrate.

Anisotropic temperature would affect the chain segment force/extension relationship as follows. Imagine the chain segment to be extended parallel to the z axis. The z component of thermal motion contributes nothing to retractive force because it averages to zero. In the case of a real chain of n atoms (with two atoms fixed) there will always be $3(n - 2)$ degrees of freedom for thermal energy. In the K/G chain there are $2n - 5$ degrees of freedom. For a fully extended chain, therefore, there are about the same number of degrees of

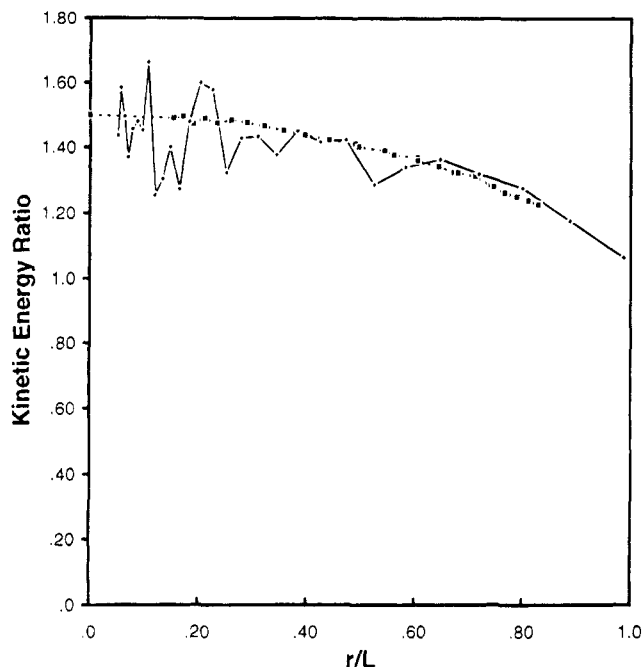


Figure 8. Anisotropy of thermal energy in chain segments represented by $\langle V^2 \rangle / \langle V_{xy}^2 \rangle$ in bond constraint models: (◆) $K = 1.35 \times 10^{-15}$ J; (■) $K = 0$.

freedom in the xy plane for the real $[2(n - 2)]$ and for the K/G chain segment $[2n - 5]$. For a chain which is hardly extended, e.g., $|r/L| \ll 1$, however, the K/G segment has fewer degrees of freedom in the xy plane, $[2(n - 2)]$ for a real vs $(4n - 10)/3$ for a K/G segment] and consequently, it seems, would not develop the same retractive force. The effects observed here are in the correct direction to explain the discrepancy in stress dependence of dynamic modulus reported by Davis,¹ but the quantitative aspects are uncertain.

The main value of this work for understanding fiber properties is probably the observation of two mechanisms which prevent the chain segment from collapsing at zero force and consequently provide for the high amorphous orientations observed in relaxed fibers. A larger effect was observed due to confining the chain segment in a tube than was reported by Weiner and Berman⁸ (Figure 5). The tube in this work was smaller, relative to the bond length, than that used by Weiner and Berman. There was no effect from the tube when the ratio of tube diameter to bond length was 3.3 or larger, which is close to the value 3.0 used by Weiner and Berman.

It was also observed that a simple intrachain stiffness also causes retractive force to become zero at a nonzero value of r/L . With a value of K thought to be appropriate for hydrocarbon chains, zero retractive force occurred when r/L was relatively large: 0.5. This is the order of zero-force chain extension reported in fully relaxed polymer fibers. In this work the stiffer the chain, i.e., the larger is K , the higher the value of r/L at which zero retractive force occurred.

Weiner and Stevens⁷ reported that the force which prevented their model from collapsing behaved somewhat like the pressure from an enclosed gas; i.e., with increasing compression, the slope of the effective force/strain relationship increases. Such behavior would impart intrinsic stability to real materials which would be highly desirable. Neither of the mechanisms for preventing network collapse observed in this work provided such stability against axial compression; i.e.,

the slope of the force/strain relationship decreases with increasing compression. Should one of the collapse-preventing mechanisms observed here represent the true process by which "amorphous" orientation is stabilized in fibers, the fibrous state of matter must be regarded as intrinsically unstable with respect to axial compression. Real, oriented polymer fibers do appear to be unstable to axial compression.

Acknowledgment. The author acknowledges helpful discussions with Dr. David Pensak and Mr. John Christy of the DuPont Co., and Drs. David Brown and Julian Clarke of UMIST. Dr. A. E. Tonelli of North Carolina State contributed helpful criticism of the manuscript. The author also acknowledges the contribution of the late Prof. P. J. Flory, who recommended pursuing the K/G route for understanding fiber physical properties.

References and Notes

- (1) Davis, H. A. *J. Text. Inst.* **1991**, 82, 86.
- (2) Nakamae, K.; Nishino, T.; Yokomaya, F.; Matsumoto, T. *J. Macromol. Sci., Phys.* **1988**, B27, 407.
- (3) Prevorsek, D. C. *J. Polym. Sci.* **1971**, C32, 368.
- (4) Gaylord, R. J. *Polym. Eng. Sci.* **1979**, 19, 955.
- (5) Kuhn, H.; Grün, W. *Kolloid Z. Z. Polym.* **1942**, 101, 248.
- (6) Davis, H. A. *J. Appl. Polym. Sci., Polym. Symp.* **1991**, 47, 143.
- (7) Weiner, J. H.; Stevens, T. W. *Macromolecules* **1983**, 16, 672.
- (8) Weiner, J. H.; Berman, D. H. *Macromolecules* **1984**, 17, 2015.
- (9) Winker, R. G.; Reineker, P. *Makromol. Chem., Macromol. Symp.* **1989**, 30, 215.
- (10) Flory, P. J. *Statistical Mechanics of Polymer Molecules*; Interscience: New York, 1969; pp 319f.
- (11) Weiner, J. H. *Statistical Mechanics of Elasticity*; Wiley: New York, 1983; pp 246–247.
- (12) Samuels, R. J. *Structured Polymer Properties*; Wiley: New York, 1974; Chapter II.
- (13) Samuels, R. J. *J. Polym. Sci.* **1965**, A3, 1741.
- (14) Dumbleton, J. H. *J. Polym. Sci., Part A-2* **1968**, 6, 796.
- (15) Brown, David Ph.D. Thesis, University of Manchester Institute of Science and Technology, 1984.
- (16) Samuels, R. J. *J. Polym. Sci., Part A-2* **1972**, 10, 781.
- (17) Davis, H. A. *Advances in Fibre Science*; Mukhopadaya, S. K., Ed.; The Textile Institute: Manchester, 1992; pp 154–155.
- (18) Helfand, E. *J. Chem. Phys.* **1979**, 71, 5000.
- (19) Fixman, M.; Kovac, J. *J. Chem. Phys.* **1974**, 61, 4939.
- (20) Hoover, W. G., *Molecular Dynamics*; Springer-Verlag: New York, 1986; Chapter 1.

MA941111J